Progress in Physics of Applied Materials 4 (2024), 183 – 188

Semnan University

Progress in Physics of Applied Materials

Journal homepage: https://ppam.semnan.ac.ir/

Structural, electronic, and magnetic properties of Fe_2TiP full-Heusler compound: A first-principles study

Reza Sarhaddi*

Department of Physics, Faculty of Sciences, University of Birjand, Birjand, Iran

ARTICLE INFO

Article history:

Received: 12 May 2024
Revised: 27 September 2024
Accepted: 2 October 2024

Keywords:

Magnetic intermetallic
Density functional theory
Half-metallic
Band structure

ABSTRACT

This study examined the electronic, magnetic, and structural properties of Fe_2TiP full-Heusler compound, using the pseudo-potential plane wave (PP-PW) formalism based on density functional theory (DFT). Energetically, the $AlCu_2Mn$-type structure of Fe_2TiP had greater stability in comparison with the $CuHg_2Ti$-type structure and showed the half-metallic (HF) ferrimagnetic behavior. Based on the results at the lattice constant of 5.65 Å, the total magnetic moment (M_{tot}) was 1 μ_B/unit cell; this finding is consistent with the Slater-Pauling (SP) rule. The minority spin band exhibited a semiconductor behavior (spin-flip gap of 0.21 eV; gap of 0.35 eV), whereas the majority spin band was metallic. The origin of half-metallicity and appearance of the minority band gap were discussed using the band structure calculations and density of states (DOS). In addition, dependence of magnetic properties on the lattice constant was evaluated. In the lattice constant range of 5.55-5.85 Å, the Fe_2TiP compound can retain the half-metallicity. Therefore, the half-metallic feature was not influenced by the lattice distortion, and this material seems to have potential applications in future spintronics devices.

1. Introduction

Given their potential use in spin-dependent electronic devices, more attention is being paid to half-metallic (HM) materials [1-5]. Among different HM materials, Heusler alloys may be suitable compounds given their high Curie temperature and compatibility with semiconductors. The chemical formula of full-Heusler alloys, as ternary intermetallic compounds, is X_2YZ (X and Y denote transition metals, and Z indicates the main group element). These compounds are crystallized in both $AlCu_2Mn$ ($L2_1$, space group Fm3m) and $CuHg_2Ti$ (space group F43m) prototypes [6, 7].

So far, various reports based on the first-principal methods have suggested full-Heusler compounds as half-metals. These compounds include Ti_2-based [8-10], Mn_2-based [11-13], Co_2-based [14-16], and Fe_2-based [17-19] alloys. In a study, Canko et al. [20] measured the electronic structure of Fe_2ZrP Heusler alloy using the first-principles full-potential linearized augmented plane wave (FP-LAPW) method and reported its HM behaviors in the $AlCu_2Mn$-type structure. In another research, Kervan et al. [21] studied the electronic structure of the Fe_2TiP Heusler compound as an isomeric compound of Fe_2ZrP, using the generalized gradient approximation (GGA) scheme within the FP-LAPW method, as it is implemented in the Wien2k package. Based on their results, Fe_2TiP is predicted to be a half-metallic ferrimagnet with a magnetic moment of 1 μ_B/f.u. and a minority-spin indirect band gap of 0.38 eV. However, they did not explain in details the origin of the half-metallicity and appearance of the minority band gap in this compound. For this reason, the motive of the present study is to re-examine the magnetic, electronic, and structural features of Fe_2TiP full-Heusler compound using the pseudo-potential plane wave (PP-PW) scheme and understand the origin of half-metallicity in this material. Since there are no experimental data available in the literature to describe the physical properties of Fe_2TiP, results of our study and relevant research [21] will promote future experimental analysis of this compound as a potential candidate for spintronic applications.

2. Computational Details

* **Corresponding author.**
E-mail address: reza.sarhaddi@birjand.ac.ir

Cite this article as:
Sarhaddi, R., 2024. Structural, electronic, and magnetic properties of Fe_2TiP full-Heusler compound: A first-principles study. *Progress in Physics of Applied Materials, 4*(2), pp 183-188. DOI: 10.22075/PPAM.2024.34112.1101

For the calculations, the PWscf code was used in the Quantum ESPRESSO software suite [22, 23]. The generalized gradient approximation (GGA) by Perdew and Wang was applied to treat the exchange-correlation potential [24]. The interactions between valence and core electrons were described with the Vanderbilt-type ultrasoft pseudopotentials [25]. For ensuring an acceptable convergence for total energy, the kinetic cutoff energy was selected to be 800 eV in the plane-wave basis set. The integration of k space in the irreducible Brillouin zone consists of a 20×20×20 k-mesh, based on the Monkhorst-Pack scheme [26]. The self-consistent convergence threshold was set to 1×10^{-8} Ry as well as the conjugate gradient (CG) algorithm during all calculations.

3. Results and Discussion

3.1. Structural Properties

For structural optimization in nonmagnetic (NM) and ferromagnetic (FM) states, we calculated the Fe_2TiP total energy (E) in $CuHg_2Ti$ and $AlCu_2Mn$-type structures as a function of the lattice constant or unit cell volume (V). Following that, the universal Murnaghan equation of state [27] was applied for the E(V) data, as shown in Figure 1.

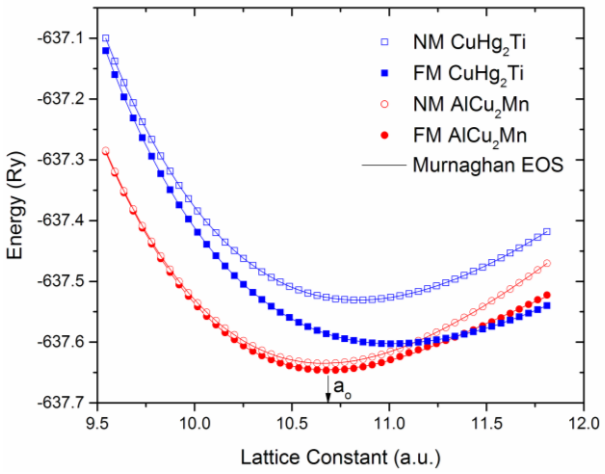

Fig. 1. Total energy of Fe_2TiP with $AlCu_2Mn$ and $CuHg_2Ti$-type structures in the NM and FM states.

As the lattice volume increases (i.e., decreasing pressure) for both crystalline structures, the energy difference increases between FM and NM phases. Moreover, a structural phase transition from $AlCu_2Mn$ to $CuHg_2Ti$ can occur as the lattice expands. Energetically, the $AlCu_2Mn$-type structure in the magnetic state is found to be the most favorable structure which in good agreement with previous report [21]; therefore, from now on, we only presented the data in the FM state for this structure. The equilibrium structural parameters, i.e., lattice constant (a_o), bulk modulus (B_o), and pressure derivative of bulk modulus (B'_o), are presented in Table 1. To our knowledge, no experimental data could be found for comparison. Nonetheless, the other theoretical data calculated by WIEN2k package based on FP-LAPW approach and also, theoretical data reported for Fe_2ZrP as the isomeric compound of Fe_2TiP are given in Table 1. It can be seen that our results, especially lattice constant, agree well with the other theoretical data [21]. However, our calculated bulk modulus and also first pressure derivative of bulk modulus underestimate their data which may be due to the different approach used in PP-PW and FP-LAPW calculations.

On the other hand, the lattice constant for Fe_2TiP in this study was 4.15% smaller than that of Fe_2ZrP, as reported by Canko et al. [20], which may be related to the greater atomic radius of Zr versus Ti (r_{Ti} = 1.462 Å, r_{Zr} = 1.603 Å) [28]. Besides, the bulk modulus of Fe_2TiP was compared with that of Fe_2ZrP; the latter showed a smaller bulk modulus, which is consistent with the relationship between the lattice constant and bulk modulus ($B_o \propto V^{-1}$; V, unit cell volume). Therefore, a lower bulk modulus is reported in compounds with a higher lattice constant. In addition, Fe_2TiP may be relatively harder than Fe_2ZrP, since bulk modulus is indicative of mechanical resistance to hydrostatic pressure. This result reflects the weaker bonding of Fe_2ZrP compared to Fe_2TiP which should be also investigated in terms of thermal stability analysis.

3.2. Thermal Stability

The enthalpy of formation (ΔH) can be used for determining the thermal stability of a Heusler compound. For the Fe_2TiP compound, ΔH is calculated considering the difference between the total energy of this compound and sum of total energies related to solid constituents (i.e., Fe, Ti, and P) at specific ground states. The following formula was used to determine ΔH:

$$\Delta H = E(Fe_2TiP) - [2E(Fe) + E(Ti) + E(P)] \quad (1)$$

Table 1 presents the ΔH value for Fe_2TiP, as well as other theoretical data. The negative value of ΔH shows that the composition of Fe_2TiP is stable thermodynamically and can be experimentally formed. In addition, the Fe_2TiP compound had a significantly larger absolute ΔH (higher stability), compared to Fe_2ZrP. This finding, besides the bulk modulus data, can be evaluated considering the electronegativity difference of titanium/zirconium with iron and phosphorus atoms (χ_{Ti} = 1.54, χ_{Zr} = 1.33, χ_{Fe} = 1.83, χ_P = 2.19) [29]. The greater difference in electronegativity of a compound results in stronger bonds [30]; therefore, a more negative ΔH is associated with a larger bulk modulus.

3.3. Electronic Structure

For determining the electronic and HM features of Fe_2TiP, the band structure of $AlCu_2Mn$-type structure was calculated for the minority and majority spins, as indicated in Fig. 2. In the majority spin state, the Fermi level passed the energy bands, indicating its metallic nature. On the contrary, a semiconducting band gap was clearly observed near the Fermi level in the minority spin state, confirming HM character of Fe_2TiP compound with the $AlCu_2Mn$-type structure.

Table 1. The equilibrium lattice constant (a_o), bulk modulus (B_o), first pressure derivative of bulk modulus (B_o'), and enthalpy of formation (ΔH) in the FM phase of Fe_2TiP compound with the $AlCu_2Mn$-type structure. The other theoretical data of Fe_2TiP and also Fe_2ZrP compound with similar crystal structure are also presented for comparison.

Compound	a_o (Å)	B_o (GPa)	B'_o	ΔH (kJ/mol)	Refs.
Fe_2TiP	5.655	228.8	4.27	-176.57	This work
Fe_2TiP	5.65	236.98	4.66	-180.43	[21]
Fe_2ZrP	5.9	202.4	4.64	-121.34	[20]

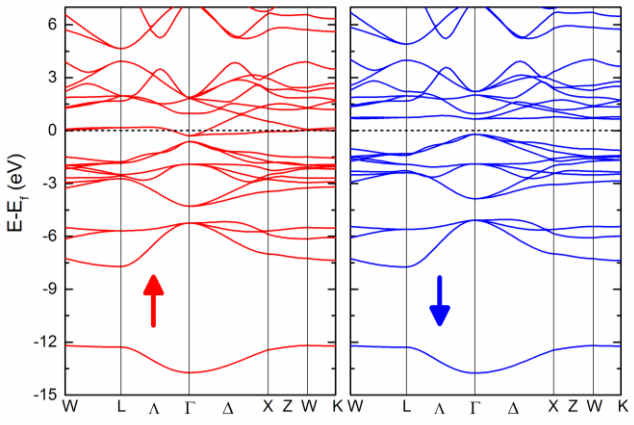

Fig. 2. The spin-polarized band structure of the Fe_2TiP compound with the $AlCu_2Mn$-type at the equilibrium lattice constant for the spin-up and spin-down channels. The dashed line presents the Fermi energy (E_F) at 0 eV.

The energy gap width was nearly 0.35 eV near the high symmetry direction Γ, which can be determined in the minority-spin channel based on the highest occupied and lowest unoccupied bands. This band gap value is in quite good agreement with 0.38 eV reported in the Kervan et al. [21] literature. However, the type of band gap observed for this compound is different: direct (Γ-Γ) and indirect (Γ-X) band gap, respectively for PP-PW and FP-LAPW approaches. Besides, valance band maximum (VBM) for minority spins is separated from Fermi level by an energy gap of 0.21 eV, i.e. the minority spin-flip gap, which marks the minimum energy required to reverse the spin of minority electrons. Since the spin-flip gap has a non-zero value, therefore, the Fe_2TiP compound with structure of $AlCu_2Mn$-type can be regarded as a "true" HM ferrimagnet (HMF).

The total and partial density of states (TDOS and PDOS, respectively) of the Fe_2TiP compound were calculated to find the origin of the minority band gap, as presented in Fig. 3. In the spin-down channel, near E_F, no PDOS was found for atoms, while the spin-up states crossed the Fermi level. Based on the spin polarization (P) formula:

$$P = \frac{N_{up}(E_F) - N_{dw}(E_F)}{N_{up}(E_F) + N_{dw}(E_F)} \qquad (2)$$

where N_{up} and N_{dw} respectively refer to the spin-up and spin-down density of states at the Fermi level), the Fe_2TiP compound exhibited spin polarization of 100% at E_F, confirming its HM feature in the equilibrium state. As a result, it can be used to produce perfect spin-polarized currents in spintronic devices.

According to Figure 3, the main contributions in energy regions between -14 and -4.5 eV originate from the s and p states of phosphorus atoms, while small contributions arise from Fe-4d and Ti-3d states. However, PDOS in the energy range -4.5 < E (eV) < 5 mostly consists of Fe-4d and Ti-3d states. In addition, TDOS of compound at Fermi energy E_F for spin-up channel are mainly attributed to Fe-d electrons.

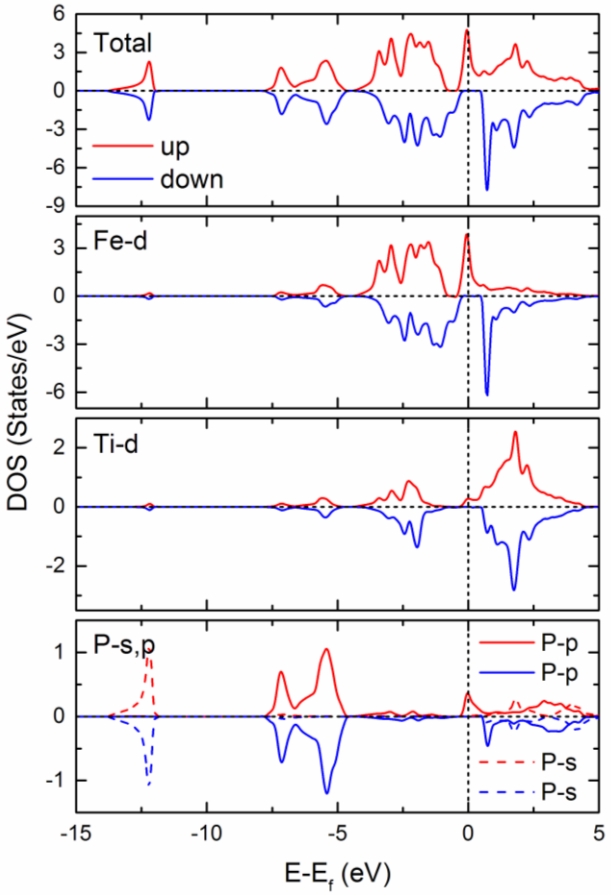

Fig. 3. TDOS and PDOS for the $AlCu_2Mn$-type structure of the Fe_2TiP compound at the equilibrium lattice constant (The zero energy indicates the Fermi level).

Although the results of the electronic structure calculations of this compound with two different pseudo- and full-potential based approaches are close together, however, the origin of the minority band gap of this compound has not been explored in the Kervan et al. [21] literature. Here, we discussed this issue in detail using the band structure calculations (Fig. 2) and density of states (Fig. 3). In both types of channels (spin-up and spin-down), the energy bands at -4.5 to 5 eV around E_F were mainly attributed to the d orbitals of iron (Fe) and titanium (Ti), hybridizing together. The three energy bands from -7.5 to -4.5 eV were mostly attributed to the p states of phosphorus (P) atom, whereas the energy band around -12 eV to the s orbitals of P atom. Therefore, among 12 minority occupied bands per unit cell for the Fe_2TiP Full-Heusler compound, one has s character, three p character, and eight d character. On the other hand, considering the PDOS of Fe_2TiP (Fig. 3), the energy gap observed in the spin-down

channel was attributed to hybridization between the 3d orbitals of Fe and Ti atoms which known as the "d-d band gap" [31]. The 3d electronic splitting of Fe atom exerted a major effect on the minority energy gap, as the gap of Fe PDOS was similar to that of TDOS of Fe_2TiP compound. Besides, the bonding states below the Fermi level were mainly from the d-states of high-valent Fe, whereas the unoccupied antibonding states were mostly in correspondence to the d-states of low-valent Ti atom. Therefore, low- and high-valent transition metal atoms showed a covalent hybridization, which resulting in an energy gap between the antibonding and bonding bands, also known as the "covalent band gap" [32]. Therefore, both d-d and covalent hybridizations were effective in the energy gap detected in the minority spin state of the Fe_2TiP compound.

3.4. Magnetic characteristics

The total (M_{tot}) and partial magnetic moments are presented in Table 2 at the equilibrium lattice constant for the $AlCu_2Mn$-type structure of the Fe_2TiP compound. Based on the findings, the M_{tot} of this compound was 1 μ_B integer value per formula unit, which is in accordance with the Slater-Pauling rule [33]. Based on this rule, the M_{tot} of a full Heusler compound is presented as N_V-24 (N_V denotes the total valence electron count in the unit cell of compound).

On the other hand, as can be seen, Fe atoms have the largest contribution to M_{tot}, while P and Ti atoms only exhibit small magnetic moment in this compound; the difference can be examined with respect to PDOS (Fig. 3). In the spin-up channel of Fe, the antibonding peak was occupied below the Fermi level, while above the Fermi level, the antibonding peak moved in the spin-down channel due to exchange splitting; this produced different electron occupations in the spin channels, therefore Fe atoms showed a large magnetic moment. Moreover, the Ti atoms magnetic moment was anti-parallel to Fe atoms, thus specifying the magnetic composition of Fe_2TiP as a ferrimagnetic compound.

Table 2. The M_{tot} and partial magnetic moment of Fe_2TiP with the $AlCu_2Mn$-type structure at equilibrium lattice constant (a_o) of 5.655 Å. The other theoretical data is also listed for comparison.

M_{tot} (μ_B)	M_{Fe} (μ_B)	M_{Ti} (μ_B)	M_P (μ_B)	Refs.
1.00	0.639	-0.287	0.009	This work
1.00	0.633	-0.151	-0.003	[21]

The lattice constant was closely associated with the stability of half-metallic feature of Heusler compounds, as variations can influence the minority or majority band gap, as well as the Fermi level relative to the band gap [34, 35]. Accordingly, using the lattice constant, the magnetic property was measured (Fig. 4).

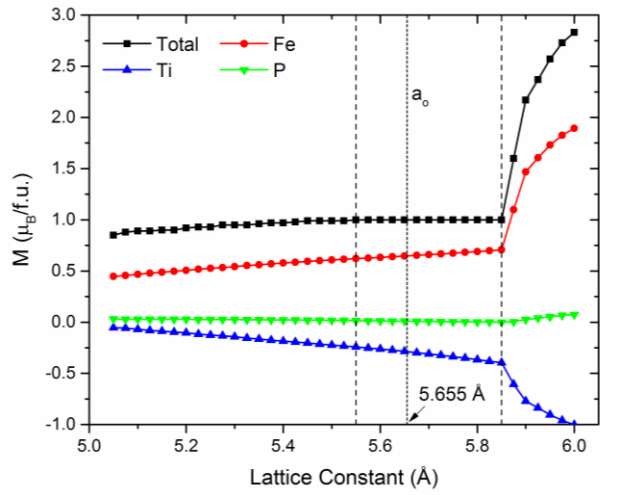

Fig. 4. The M_{tot} of Fe, Ti, and P atoms in relation to the lattice constant. The short and long vertical dashed lines represent the equilibrium lattice constant (a_o) and the half-metallicity range for Fe_2TiP, respectively.

Evidently, in a broad range of the lattice constant, the M_{tot} was 1 μ_B integer value. Based on the findings, a moderate shift in the lattice constant cannot cause a significant change in M_{tot}. By reducing the lattice constant or improving pressure on the lattice, M_{tot} slowly reduced to < 1 μB; therefore, the half-metallic property of Fe_2TiP disappeared. Nevertheless, the absolute partial magnetic moment of Fe and Ti atoms improved as the lattice constant increased, whereas the lattice distortion did not influence the magnetic moment of P. An explanation can be presented for this finding. Expansion of the lattice constant reduces the electron cloud overlap, thus deteriorating the hybridization of d states in transition metals, improving the exchange splitting in d states, and increasing the magnetic moment of Fe and Ti. With increasing lattice constants to values greater than 5.85 Å, hybridization between neighboring atoms decreases and the behavior of atoms tends toward isolated atoms which enhances their magnetization [36].

A similar behavior was reported by Kervan et al. [21] for Fe_2TiP and Canko et al. [20] for Fe_2ZrP compound. Moreover, the ferrimagnetic Fe_2TiP compound maintains its half-metallic characteristic at the lattice constant range of 5.55 to 5.85 Å. Considering this stability in a wide region, this material is useful for spintronic applications.

4. Conclusions

We employed the first-principles calculations, using the PWscf code in GGA-PW91 to examine the electronic structure, magnetic features, and stability of the Fe_2TiP compound. The results showed that the $AlCu_2Mn$-type structure was ferrimagnetic with half-metallic characteristics and at the Fermi level, it exhibited 100% spin polarization, while the $CuHg_2Ti$-type structure showed conventional ferromagnetic behaviors. The M_{tot} was 1.00 μ_B/f.u. per unit cell, following the Slater-Pauling rule (M_{tot}= N_V-24) for a broad range of the lattice constant. Based on the findings, the minority band gap may originate from the covalent and d-d hybridizations of Fe and Ti transition metals.

Acknowledgments

There is nothing to acknowledgement.

Conflicts of Interest

The author declares that there is no conflict of interest regarding the publication of this article.

References

[1] Dho, J., Ki S., Gubkin, A.F., Park, J.M.S., Sherstobitov, E.A., 2010. A neutron diffraction study of half-metallic ferromagnet CrO_2 nanorods. Solid State Commun. 150, pp. 86-90.

[2] Zhu, Z.H., Yan, X.H., 2009. Half-metallic properties of perovskite $BaCrO_3BaCrO_3$ and $BaCr_{0.5}Ti_{0.5}O_3BaCr_{0.5}Ti_{0.5}O_3$ superlattice: LSDA+U calculations. J. Appl. Phys. 106, pp. 023713.

[3] Kronik, L., Jain, M., Chelikowsky, J.R.: Electronic structure and spin polarization of $Mn_xGa_{1-x}N$. Phys. Rev. B. 66, 041203 (2002).

[4] Kobayashi, K.L., Kimura, T., Sawada, H., Terakura, K., Tokura, Y., 1998. Room-temperature magnetoresistance in an oxide material with an ordered double-perovskite structure. Nature 395, pp. 677-680.

[5] de Groot, R.A., Mueller, F.M., van Engen, P.G., Buschow, K.H.J., 1983. New Class of Materials: Half-Metallic Ferromagnets. Phys. Rev. Lett. 50, pp. 2024-2027.

[6] Kervan, N., 2012. Half-metallicity in the full-Heusler Co_2ScP compound: A density functional study. J. Magnet. Magnet. Mater. 324, pp. 4114-4117.

[7] Kandpal, H.C., Fecher, GH, Felser, C., 2007 Calculated electronic and magnetic properties of the half-metallic, transition metal based Heusler compounds. J. Phys. D: Appl. Phys. 40, pp. 1507.

[8] Wei, X.P., Zhang, Y.L., Sun, X.W., Song, T., Guo, P., 2016. The electronic and magnetic properties of defects on half-metallic Ti_2NiIn alloy. J. Solid State Chem. 233, pp. 221-228.

[9] Qi, S., Shen, J., Zhang, C.H., 2015. First-principles study on the structural, electronic and magnetic properties of the Ti_2VZ (Z = Si, Ge, Sn) full-Heusler compounds. Mater. Chem. Phys. 164, pp.177-182.

[10] Wei, X.P., Deng, J.B., Mao, G.Y., Chu, S.B., Hu, X.R., 2012. Half-metallic properties for the Ti_2YZ (Y= Fe, Co, Ni, Z= Al, Ga, In) Heusler alloys: A first-principles study. Intermetallics 29, pp. 86-91.

[11] Anjami, A., Boochani, A., Elahi, S.M., Akbari, H., 2017. Ab-initio study of mechanical, half-metallic and optical properties of Mn_2ZrX (X = Ge, Si) compounds. Results Phys. 7, pp. 3522-3529.

[12] Kervan, N., Kervan, S., Canko, O., Atiş, M., Taşkin, F., 2016. Half-metallic Ferrimagnetism in the Mn_2NbAl full Heusler compound: A first-Principles study. J. Supercond. Novel Magn. 29, pp. 187-192.

[13] Li, S.T., Ren, Z., Zhang, X.H., Cao, C.M., 2009. Electronic structure and magnetism of Mn_2CuAl: A first principles study. Phys. B: Condens. Matter. 404, pp. 1965-1968.

[14] Rai, D.P., Shankar, A., Sandeep Ghimire, M.P., Thapa, R.K., 2013. Electronic and magnetic properties of a full-Heusler alloy Co_2CrGe: a first-principles study. J. Theo. App. Phys. 7, pp. 3.

[15] Zareii, S.M., Arabi, H., Sarhaddi, R., 2012. Effect of Si substitution on electronic structure and magnetic properties of Heusler compounds $Co_2TiAl_{1-x}Si_x$. Phys. B: Condens. Matter. 407, pp. 3339-3346.

[16] Gökoglu, G., 2010. First principles electronic structure calculations of Co_2CrBi Heusler system. Phys. B: Condens. Matter. 405, pp. 2162-2165.

[17] Dahmane, F., Mogulkoc, Y., Doumi, B., Tadjer, A., Khenata, R., Bin Omran, S., Rai, D.P., Murtaza, G., Varshney, D., 2016. Structural, electronic and magnetic properties of Fe_2-based full Heusler alloys: A first principle study. J. Magnet. Magnet. Mater. 407, pp. 167-174.

[18] Chen, B.S., Li, Y.Z., Guan, X.Y., Wang, C., Wang, C.X., Gao, Z.Y., 2015. First-principles study of half-metallic and magnetic properties for the Heusler alloys Fe_2CrX (X= P, As, Sb, Bi). J. Supercond. Novel Magn. 28, pp. 1559-1564.

[19] Luo, H.Z., Zhu, Z.Y., Ma, L., Xu, S.F., Liu, H.Y., Qu, J.P., Li, Y.X., Wu, G.H., 2007. Electronic structure and magnetic properties of Fe_2YSi (Y= Cr, Mn, Fe, Co, Ni) Heusler alloys: a theoretical and experimental study. J. Phys. D: Appl. Phys. 40, pp. 7121.

[20] Canko, O., Taskin, F., Atis, M., Kervan, N., Kervan, S., 2016. Magnetism and half-metallicity in the Fe_2ZrP Heusler alloy. J. Supercond. Novel Magn. 29, pp. 2573-2578.

[21] Kervan, N., Kervan, S., 2013. Half-metallic properties in the Fe_2TiP full-Heusler compound. Intermetallics 37, pp. 88-91.

[22] Giannozzi, P. et al., 2009. QUANTUM ESPRESSO: a modular and open-source software project for quantum simulations of materials. J. Phys.: Condens. Matter. 21, pp. 395502.

[23] Giannozzi, P. et al., 2017. Advanced capabilities for materials modelling with Quantum ESPRESSO. J. Phys.: Condens. Matter., 29, pp. 465901.

[24] Perdew, J.P., Chevary, J.A., Vosko, S.H., Jackson, K.A., Pederson, M.R., Singh, D.J., Fiolhais, C., 1992. Atoms, molecules, solids, and surfaces: Applications of the generalized gradient approximation for exchange and correlation. Phys. Rev. B 46, pp. 6671.

[25] Vanderbilt, D., 1990. Soft self-consistent pseudopotentials in a generalized eigenvalue formalism. Phys. Rev. B, 41, pp. 7892.

[26] Monkhorst, H.J., Pack, J.D., 1976. Special points for Brillouin-zone integrations. Phys. Rev. B 13, pp. 5188.

[27] Murnaghan, F.D., 1944. The Compressibility of media under extreme pressures. Proc. Natl. Acad. Sci. 30, pp. 244.

[28] Guo, S., Liu, C.T., 2011. Phase stability in high entropy alloys: formation of solid-solution phase or amorphous phase. Progr. Nat. Sci.: Mater. Int. 21, pp. 433-446.

[29] McNaught, A.D., Wilkinson, A., Compendium of Chemical Terminology. Blackwell Science, Oxford, 1997.

[30] Sarhaddi, R., Arabi, H., Pourarian, F., 2014. Structural, stability and electronic properties of C15-AB_2 (A= Ti, Zr; B = Cr) intermetallic compounds and their

hydrides: An ab initio study. Int. J. Mod. Phys. B. 28, pp. 1450105.
[31] Ahmadian, F., 2014. Half-metallicity in a new Heusler alloy Ti_2FeSn: A density functional study. J. Korean Phys. Soc. 64, pp. 277-282.
[32] Kandpal, H.C., Felser, C., Seshadri, R., 2006. Covalent bonding and the nature of band gaps in some half-Heusler compounds. J. Phys. D: Appl. Phys. 39, pp. 776-785.
[33] Galanakis, I., Dederichs, P.H., Papanikolaou, N., 2002. Slater-Pauling behavior and origin of the half-metallicity of the full-Heusler alloys. Phys. Rev. B 66, pp. 174429.
[34] Feng, L., Liu, E.K., Zhang, W.X., Wang, W.H., Wu, G.H., 2014. First-principles investigation of half-metallic ferromagnetism of half-Heusler compounds XYZ. J. Magnet. Magnet. Mater. 351, pp. 92-97.
[35] Block, T., Carey, M.J., Gurney, B.A., Jepsen, O., 2004. Band-structure calculations of the half-metallic ferromagnetism and structural stability of full- and half-Heusler phases. Phys. Rev. B 70, pp. 205114.
[36] Sadeghi, K.H., Ahmadian, F., 2004. Half-metallic ferromagnetism in Ti_2IrZ (Z = B, Al, Ga, and In) Heusler alloys: A density functional study. Pramana-J. Phys. 90, pp. 1-11.